Phase stability of long-period stacking structures in Mg-Y-Zn: A first-principles study

Phase stability of long-period stacking structures in Mg-Y-Zn: A first-principles study

Satoshi Iikubo,[1,2] Kensuke Matsuda,[3] and Hiroshi Ohtani[4,2]

[1]*Graduate School of Life Science and Systems Engineering, Kyushu Institute of Technology, Kitakyushu 808-0196, Japan*

[2]*JST, CREST, Tokyo, 102-0075, Japan*

[3]*Graduate School, Kyushu Institute of Technology, Kitakyushu 804-8550, Japan*

[4]*Department of Materials Science and Engineering, Kyushu Institute of Technology, Kitakyushu 804-8550, Japan*

(Received 6 February 2012; revised manuscript received 7 July 2012; published 3 August 2012)

The phase stability of the long periodic structures in Mg has been investigated at finite temperature by means of first-principles calculations. Free-energy calculation, including the lattice vibration effect, clearly reveals that 14H and 18R type long periodic structures become more stable than 2H-Mg. Furthermore, the stacking fault energies from a structure of ABA (hcp) to ABC (fcc) were calculated for the isotropic lattice variation. We found that the stacking fault energy decreased by lattice expansion and went to nearly zero upon 10% expansion of the lattice. These two calculated results provide important information about the formation of long periodic stacking "ordered" (LPSO) structures in a Mg-Y-Zn system. It has been suggested that the substituted large atoms and temperature effect cooperatively generate a metastable long periodic stacking faults structure that precede LPSO formation.

DOI: 10.1103/PhysRevB.86.054105 PACS number(s): 63.20.D−, 63.20.Ry, 64.60.My

I. INTRODUCTION

Magnesium-based alloys are attractive for many structural engineering applications owing to their low density and high specific strength. Among them, the recently discovered long-period stacking ordered (LPSO) Mg alloys have been reported to show a yield strength of 610 MPa and elongation of 5% at room temperature as well as high thermal stability.[1] In addition to the excellent mechanical properties, the characteristic crystal structure also attracts attention from the viewpoint of fundamental science. LPSO-Mg is formed by the periodical arrangement of a stacking fault (SF) based on the hcp lattice. Furthermore, the substituted rare-earth and transition metal atoms form two atomic layers in the stacking fault site. Because long periodic structures seem to induce remarkable structural strength concomitant with a series of exotic properties, a precise understanding of the LPSO structure formation is of vital importance not only for revealing the stability of the basic structures, but also for tailoring material functionality.

Many theoretical models have been concerned with the stacking fault transformation in metals and alloys. Most of them focus on the transformation mechanism between two close-packed structures described in terms of nucleation and growth processes.[2–5] Other approaches are formulated in terms of shearing mechanisms or Fermi surface mechanisms taking into account the average electron concentration per atom.[6] In the present study, we focus on the effect of finite temperature on structural phase transition. Because the entropy of lattice vibration may play an important role in the phase transformation at $T \neq 0$, a different result can be expected from the calculation at $T = 0$. Recent experimental results reported that the LPSO structure can be varied depending on the temperatures of heat treatment,[7] and this finding suggests that temperature is an important parameter for understanding the SF formation. Furthermore, previous studies also suggested that the SF formation strongly correlates with the lattice constant. Even in pure rare-earth (RE) metals, crystal structures are known to show the sequence hcp → Sm-type → double-hcp → fcc for decreasing atomic number and increasing pressure. Kawamura *et al.* discussed the criteria for the formation of the LPSO phase in Mn-Zn-RE alloys from the viewpoints of the solid solubility limit of RE elements in Mg, and the difference in atomic size between Mg and RE elements.[8] Because introduced large atoms seem to expand the crystal lattice locally, the effect of lattice expansion on the SF formation must be understood accurately.

The purpose of the present study is to examine the transformation behavior in terms of temperature and lattice expansion by means of a first-principles calculation. First-principles phonon calculations of the long periodic structures are carried out to calculate the vibrational contributions to the total free energy and finite temperature thermodynamic properties. Based on our detailed calculation of the SF formation at the atomic level, we propose "disordered" long periodic structures as a preliminary step in LPSO formation.

II. CALCULATION PROCEDURES

The total energy calculations were performed with the VASP code,[9,10] which is based on the density functional theory. Exchange and correlation functions were given by the generalized gradient approximation as proposed by Perdew *et al.*[11] The electron-ion interaction was represented by the projector augmented wave method with plane waves up to an energy of 400 eV (Ref. 12). The k-point meshes of Brillouin zone sampling in a primitive cell were based on the Monkhorst-Pack scheme[13] with Fermi broadening of 0.2 eV. The actual value of the k-point meshes were $24 \times 24 \times 16$ for 2H, $24 \times 24 \times 8$ for 4H, $24 \times 24 \times 6$ for 6H, $24 \times 24 \times 4$ for 9R, $24 \times 24 \times 2$ for 10H, $24 \times 24 \times 1$ for 14H, and $24 \times 24 \times 1$ for 18R. The convergence criteria for energy and force were 0.1 meV and 0.02 eV/Å, respectively. Structural optimizations were re-initiated at least two times.

Dynamical properties were obtained from the direct method.[14] In this method, phonon frequencies were calculated from Hellmann-Feynman (HF) forces generated by nonequivalent atomic displacement in a supercell for a crystal structure. In the present study, the dimensions of supercells

were $3 \times 3 \times 2$, $3 \times 3 \times 1$, $3 \times 3 \times 1$, $3 \times 3 \times 1$, $3 \times 3 \times 1$, $3 \times 3 \times 1$, and $3 \times 3 \times 1$ of their unit cells for 2H, 4H, 6H, 9R, 10H 14H, and 18R, respectively. For the calculation of those large systems, k-point sampling is limited to 0.15 per Angstrom, for example, $6 \times 6 \times 1$ mesh for 18R. A dynamical matrix was constructed from HF forces acting on all atoms in supercells with a displaced atom and phonon frequencies were calculated by solving the eigenvalue problem for the dynamical matrix. Thermal expansion was indirectly taken into account through calculations for various lattice volumes.

III. RESULTS AND DISCUSSION

A. Phase stability of long period structures

Figure 1 shows the atomic arrangement of 2H, 4H, 6H, 9R, 10H, 14H, and 18R structures. A hexagonal close-packed structure (hcp) is specified by ABABAB, and a face-centered cubic structure (fcc) is described by ABCABC, where A, B, and C are three atomic sites. Other long periodic structures are described as follows: 4H:d-hcp with stacking, A|BA|C; 6H with stacking, AB|ACA|B; 9R with stacking, AC|ABA|BCB|CA; 10H with stacking, AC|BABAB|C; 14H with stacking, ACAC|BABABAB|CAC; and 18R with stacking, ACAC|BABABA|CBCBCB|AC, where the stacking fault planes are denoted by bars. Although various experimental techniques have revealed that there are different stacking sequences in each structure, in this study, we employ the above-mentioned stacking sequences for simplicity. Among them, 4H and 6H are denoted by the intrinsic fault I_1 and 10H, 14H, and 18R are denoted by the I_2 in the previous work.[15] A convenient way to intuitively recognize these structures is to consider the structure as an aggregation of 2H blocks (ABAB, . . . ,) with stacking faults (ABC) between them. The atomic numbers of each block are 2, 3, 3, 5, 7, and 6 for 4H, 6H, 9R, 10H, 14H, and 18R, respectively. In this manner, several

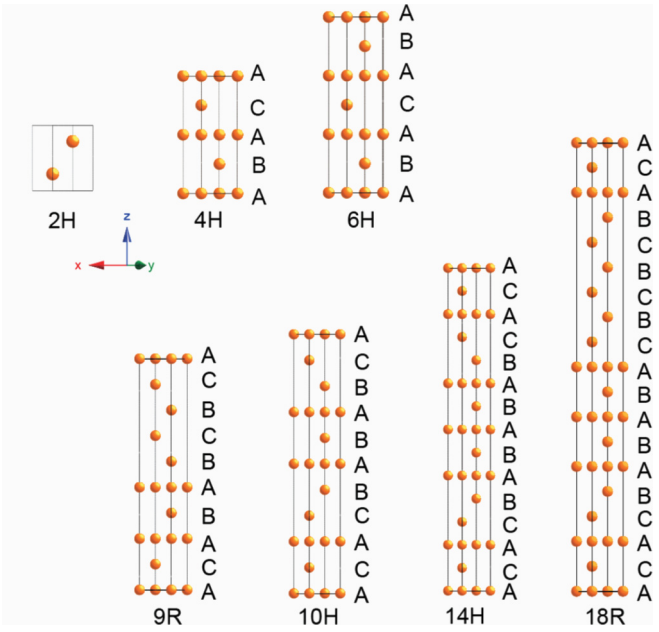

FIG. 1. (Color online) Different layered structures of Mg. A, B, and C show the atomic sites in the hcp lattice.

TABLE I. Calculated structural parameters of a unit cell and energy of formation per mole of atom for 2H, 4H, 6H, 9R, 10H, 14H, and 18R.

Phase	Lattice parameters a(Å)	c(Å)	c/c_{2H}	Energy of formation E_{form} (kJ/mol)
2H	3.199	5.196	1	
4H	3.200	10.406	2.003	0.5568
6H	3.200	15.601	3.003	0.3658
9R	3.201	23.370	4.498	0.2870
10H	3.202	25.971	4.999	0.3774
14H	3.199	36.314	6.989	0.2672
18R	3.202	46.734	8.995	0.3386

classes of metals are known to adopt a structure that can be regarded as a compromise between fcc and hcp blocks.

The total energy optimizations were conducted for these different stacking structures of Mg. Lattice constants and internal positions in primitive cells were fully optimized. The optimized lattice constants and total energy per mole of an atom at the ground state are presented in Table I. The calculated value of the lattice constant for a 2H structure was found to be $a = 3.199$ Å, $c = 5.196$ Å. These values agree well with the experimental values of $a = 3.2125(5)$ Å, $c = 5.2132(8)$ Å (Ref. 16), and with the calculated results of 3.21 and 5.20 by Wu *et al.*[17] The experimental lattice constant for an 18R structure is also reported at the X-Mg_{12}ZnY phase to be $a = 3.224$ Å, $c = 46.985$ Å (Ref. 18), which is in good agreement with the calculated values $a = 3.202$ Å and $c = 46.734$ Å for 18R in this study.

Table I also shows the values of the energy of formation E_{form}. The positive values of E_{form} for all structures indicate that an introducing stacking fault into 2H-Mg causes the system to destabilize at $T = 0$. The energetic hierarchy of Mg polymorphs is 4H > 10H > 6H > 18R > 9R > 14H, as shown in Table I. This result is partly in agreement with the previous study, ranking the total equilibrium energy as two-layer (hcp), six-layer, four-layer (d-hcp), and three-layer (fcc) in ascending order.[19]

Next, to obtain a fully relaxed state at various volumes of the anisotropic system, structures are optimized under an external pressure of $P = 7, 5, 2, 0, -3, -5$, and -6 GPa. For example, the inset of Fig. 2 shows the pressure dependence of the energy of formation for 2H and 18R structures. Although the inset does not show a discernible difference between 2H and 18R, we can see a clear tendency of volume dependence on the energy difference between the long periodic structures and 2H, as shown in the main panel of Fig. 2. Although each behavior is too involved a subject to be treated here in detail, the values of the energy difference monotonically decrease with increasing volume for all structures. An important feature is that the energy difference becomes smaller, and thus the structures including the stacking fault become stable with volume expansion. The pressure dependence of phase stability between the fcc and hcp of Mg has been studied previously.[20] Our calculation is consistent with their results on the volume dependence under pressure or volume contraction.

To investigate phase stability at a finite temperature the contribution of the free energy of harmonic and anharmonic

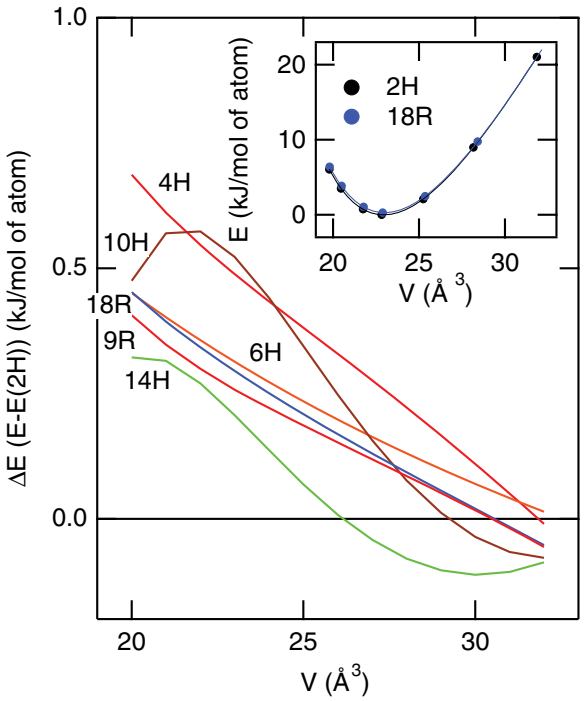

FIG. 2. (Color online) Volume dependence of the energy difference between each long periodic structure and 2H. The inset shows the volume dependence of the energy of formation calculated for 2H and 18R.

effects on the lattice vibration must be considered. To estimate the lattice contribution we used the quasiharmonic approximation. The quasiharmonic approximation provides a reasonable description of the thermodynamic properties of simple metals[21,22] and other ceramics[23–25] below their melting points. The vibrational free energy of the lattice ions $F^{\mathrm{ph}}(V,T)$ is

$$F^{\mathrm{ph}}(V,T) = E(V) + k_B T \sum_{\mathbf{q}} \sum_{j} \ln \left\{ 2 \sinh \left[\frac{\hbar \omega_j(\mathbf{q},V)}{2 k_B T} \right] \right\}, \tag{1}$$

where $E(V)$ is the energy of the static lattice at a given volume V and $\omega_j(\mathbf{q},V)$ is the frequency of the jth phonon band at point $\mathbf{q}$ in the Brillouin zone. A quasiharmonic approximation, assuming that phonon frequencies depend only on the cell parameters, was employed here. This enabled us to take thermal expansion into account.

Figure 3 shows the phonon density of states (PDOS) calculated for 2H and 18R. The dispersion curve of the phonon of all structures is composed of a real frequency except for the small imaginary frequency of the transverse acoustic mode at the vicinity of point Γ. These imaginary frequencies are likely an error in a phonon calculation based on the force constant in the supercell model.[26] Since the magnitude of the imaginary frequencies are quite small, we may say that the ambiguity of thermodynamic quantities calculated from the PDOS can be ignored.

The PDOS for both structures mainly distributes below 8 THz and has a sharp peak at 7 and 4 THz. The two calculations agree well with each other, although the whole spectrum of 18R moves to smaller frequencies compared with those of 2H.

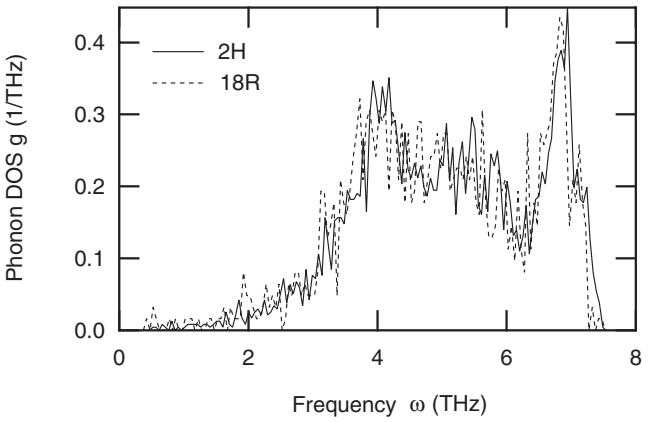

FIG. 3. Phonon density of states (PDOS) in 2H and 18R structures.

Figure 4 shows a plot of the vibrational free energy F^{ph} for 2H and 18R structures calculated with the PDOS. These figures are denoted by a lattice volume at temperatures from 0 to 1700 K. It must be noted that the results above the melting point $T = 923$ K may not have sufficient accuracy for detailed discussion because the validity of the quasiharmonic approximation decreases close to the melting point. To relate the vibrational free energy $F^{\mathrm{ph}}(V,T)$ and thermal properties, the third-order Birch-Murnaghan equation of state[27] was used. The lattice volumes with minimum free energy were determined from the fitting at each temperature, given by the solid lines in Fig. 4. As shown in this figure, the lattice volume for both the structures increases with increasing temperature. For 2H, the lattice volume of the minimum free energy is 23.088 Å^3 at 0 K, and substantially increases to 31.862 Å^3 at 1700 K, whereas for 18R, the figure shows that the lattice volume of the minimum free energy is 23.185 Å^3 at 0 K and substantially increases to 30.674 Å^3 at 1700 K, as shown in Fig. 4(b). It is difficult to estimate the minimum free energy above 1700 K because the system exhibits the anomalous behavior due to the softening of the phonon. By these means, we can obtain Helmholtz free energy based on quasiharmonic approximation, including the entropy of vibration at a finite temperature, from PDOS with various lattice volumes V.

Figure 5 shows the plots of the differences in Helmholtz free energy ΔFs compared with the 2H structure. Solid-solid phase transformation can be discussed with Helmholtz free energy instead of Gibbs free energy at an ambient pressure because volume change is very small. Among them, ΔFs of 4H, 6H, 9R, and 10H structures have positive value at $0 < T <$ 1500 K and do not show any sign change. This result means that these structures are unstable relative to the 2H structure. On the other hand, we can see obvious sign changes in the ΔFs of 14H and 18R structures. From Fig. 5, the transformation temperature can be found to be approximately 400 and 600 K for 18R and 14H, respectively. Above these temperatures, long-period structures become relatively stable compared to the 2H structure.

We have good reason for thinking that the change in the atomic bonding state plays a significant role in the structural phase transition between 2H–18R and 2H–14H. The Mg–Mg bonds in 2H-Mg are expected to be stiffer than those in the

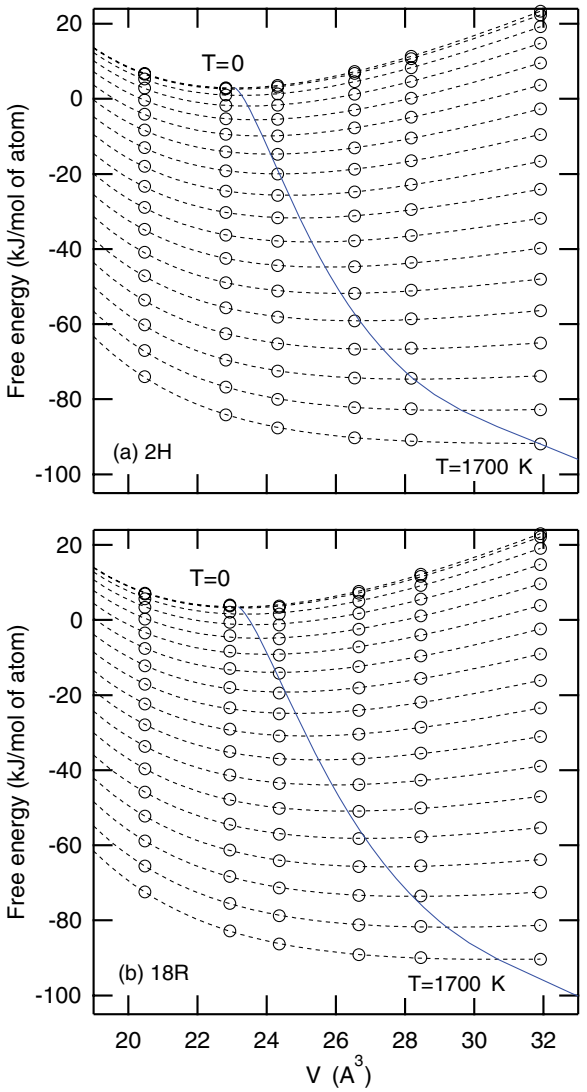

FIG. 4. (Color online) Plots of Helmholtz free energy F per formula unit against lattice volume V per formula unit from 0 to 1700 K at every 100 K for (a) 2H and (b) 18R. Dashed lines are F-V fitting curves according to the third-order Burch-Murnaghan equation of states. The solid line connects minimum energy points at each temperature.

long periodic structures having stacking fault. Because the stiff bonds move the phonon spectrum toward a higher frequency region, the energy shift of PDOS between 18R and 2H occurs, as shown in Fig. 3. The increase in energy of PDOS for 2H-Mg causes the vibrational entropy of 2H-Mg at finite temperature to be lower than that of long-period structures. Therefore, it is expected that the vibrational entropy becomes larger as the number of stacking faults increases in the unit cell.

For 4H, 6H, and 9R, ΔFs does not decrease with increasing temperature; thus, the gain of vibrational entropy seems small. On the other hand, the ΔF of 10H decreases as temperature increases. However, ΔF does not demonstrate sign change because the vibration entropy has a small contribution. Finally, 14H and 18R structures have a low critical transformation temperature. Therefore, it can be concluded that the key factor of sign change of ΔFs at elevated temperatures originates in

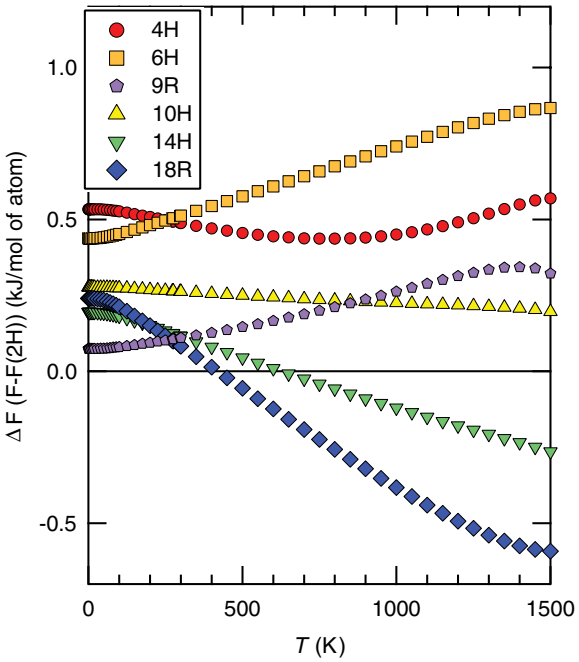

FIG. 5. (Color online) Temperature dependence of the difference in Helmholtz free energy ΔF between each long periodic structure and 2H.

the effect of lattice vibration. These results suggest that long periodic structures with stacking fault are more stable than 2H structures at high temperature.

We also point out that the thermal expansion effect included in our phonon calculation is another important factor. We have already demonstrated that lattice expansion will stabilize long periodic structures even at $T = 0$. Lattice expansion is expected to originate from both the introduction of a large atom and the thermal effect. The correspondence between the results of $T = 0$ and $T \neq 0$ implies that volume expansion makes the long-period structures stable, whether the origin is the chemical pressure or the thermal effect.

B. Transformation path for generating stacking fault

Next, we will focus on the detailed transformation path from normal stacking to stacking fault. To investigate stacking fault energy, a simple isolated system formed by Mg atoms is prepared. The long periodic structures, for example, the 4H structure, consists of successive stacking of close-packed layers with the periodic sequence $\cdots$ A|BA|C $\cdots$, while the hcp structure has the stacking sequence $\cdots$ ABABAB $\cdots$. Consider a three-atom system, as shown in Fig. 6(a), which shows ABA normal stacking. Concerning the transformation path from ABA to ABC, the stacking sequence of close-packed atomic planes is transferred by shifting the third atomic planes in the 1/3[1–100] direction, which is indicated by the arrow in Fig. 6(b). The total energy for the different atomic positions is calculated by first-principles calculations. To investigate energy variation on the given local structure, we calculate the stacking fault energy without performing internal relaxations. A calculated result is shown in Fig. 6(b) as contour plots. The maximum and minimum energies are located at (1/3, 2/3) in fractional coordinates, as denoted by B, and at (2/3, 1/3), as

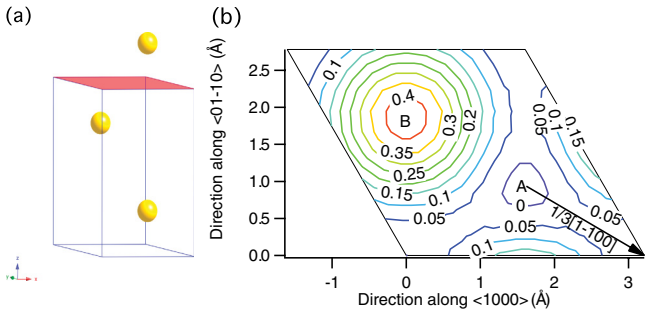

FIG. 6. (Color online) (a) Simple isolated system containing three Mg atoms. (b) Change of the contour maps of total energy projected on the c plane, where the contour lines are drawn for counts of less than 0.4 (eV) with a separation of 0.05 (eV). The energy map is calculated by fixing the lower two atoms and shifting the top atom displayed in (a).

denoted by A, respectively. Here the stacking fault energy is determined as the difference in energies from those of the ABA structure. In addition, we introduce a scale factor s of the lattice constant to control the system volume. Therefore the unit cell volume is described by $V = a_{2H} \times \sqrt{3}/2 \cdot b_{2H} \times c_{2H} \times (s)^3$.

Figure 7 shows the stacking fault energy for scale factor $s = 0.9$, 0.95, 1.0, 1.05, and 1.1. Vector d represents an atom displacement in the atoms in the top atom in the 1/3[1–100] direction. Here $d = 0$ corresponds to the ABA structure, while $d = 1$ to the ABC structure. The energy maximum encountered along the 1/3[1–100] direction represents the lowest energy barrier for shifting the atomic planes. The energy minimum at the final position 1/3[1–100] corresponds to the stable stacking fault configuration. For a scale factor of 1.0, the calculated value of the stacking fault energy was found to be 36.6 mJ/m^2. The results of the VASP calculations of stacking fault energies in Mg are in broad agreement with some previous calculations.[15,17,28,29]

We turn to the volume dependence of the stacking fault energy, which increases with decreasing scaling factor, as shown in Fig. 7. For contraction, the stacking fault energy increases and reaches almost 100 mJ/m^2 at $d = 1.0$ for $s = 0.9$. For expansion, however, the figure shows that the

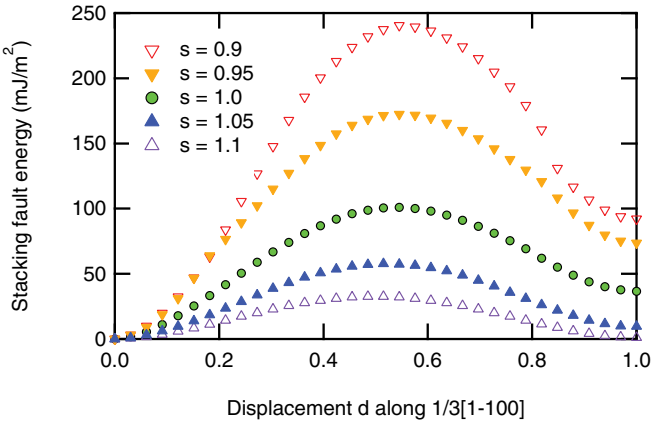

FIG. 7. (Color online) Stacking fault energy as a function of the absolute value of displacement vector $d = 1/3[1-100]$ along the ABA-to-ABC deformation path.

stacking fault energy at $d = 1.0$ is almost negligible for $s = 1.1$. These results agree with our previous calculations that the stacking fault generation in Mg is likely to occur with increasing lattice expansion. However, for $s = 1.1$, the energy maximum, which is the unstable stacking fault energy, remains finite at a value of about 30 mJ/m^2. This means that the system retains a finite energy barrier for the shifting of the atomic planes, even if structures introduced by the stacking fault become stable. To the best of our knowledge, the 18R–2H or 14H–2H transformation of pure Mg has not been observed experimentally. Estimated transformation temperatures from free energies are about 400 and 600 K, while the melting temperature is $T = 650\,^{\circ}$C (923 K). Although the transformation may be observed in future by more careful observation, we would like to point out that this finite energy barrier may disturb the introduction of the stacking fault into pure Mg.

Finally, we would like to discuss the elementary step of LPSO formation. Our calculation results, which include the lattice vibration effect, indicate that pure Mg retains structural transformation instability from hcp to other long periodic structures in the finite temperature region, even if the system is not under any external effects. In addition, the introduction of large-radius atoms such as rare-earth elements, can accelerate the tendency of phase transition toward long periodic structures because the hcp lattice is locally expanded by the introduced atoms. In a practical process of synthesis, after the solution treatment, the α (hcp) phase will precipitate as temperature decreases. This precipitation will promote the condensation of substitution atoms in the remnant part of the system. Further lattice expansion can trigger structural transformation. Our investigation strongly suggests that as a precursor of LPSO-Mg, long periodic "disordered" structures, like martensite, are formed in Mg solid solutions with the introduction of large atoms.

IV. CONCLUSION

First-principles total energy calculations within the density functional theory were performed to understand the energetics of various layered structures of Mg to address the unresolved issues related to the unique structures. The free energy calculation that included the lattice vibration effect clearly reveals that 14H and 18R type long periodic structures become more stable than 2H-Mg. Furthermore, we discovered that the stacking fault energy was decreased by the lattice expansion and goes to nearly zero by 10% expansion of the lattice. These two calculated results give us important information about the formation of long periodic stacking "ordered" Mg alloy, discovered in the Mg-Y-Zn system. The results suggest that the substituted large atoms and temperature effect cooperatively generate a metastable long periodic "disordered" structure before LPSO formation.

ACKNOWLEDGMENTS

This work was partly supported by the Grant-in-Aid for Scientific Research on Innovative area (2308) from the Japanese Ministry of Education, Culture, Sports, Science, and Technology.

[1]M. Yamasaki, M. Sasaki, M. Nishijima, K. Hiraga, and Y. Kawamura, Acta Mater. **55**, 6798 (2007).
[2]D. Pandey and S. Lele, Acta Metall. **34**, 415 (1986).
[3]S. Mahajan, M. Green, and D. Brasen, Metall. Mater. Trans. A **8**, 283 (1977).
[4]W. Bollmann, Acta Metall. **9**, 972 (1961).
[5]H. Fujita and S. Ueda, Acta Metall. **20**, 759 (1972).
[6]R. Bruinsma and A. Zangwill, Phys. Rev. Lett. **55**, 214 (1985).
[7]J. Lee, K. Sato, T. J. Konno, and K. Hiraga, Mater. Trans. **50**, 222 (2009).
[8]Y. Kawamura and M. Yamasaki, Mater. Trans., JIM **48**, 2986 (2007).
[9]G. Kresse and J. Furthmüller, Phys. Rev. B **54**, 11169 (1996).
[10]G. Kresse and J. Furthmüller, Comput. Mater. Sci. **6**, 15 (1996).
[11]J. P. Perdew, K. Burke, and M. Ernzerhof, Phys. Rev. Lett. **78**, 1396 (1997).
[12]P. E. Blöchl, Phys. Rev. B **50**, 17953 (1994).
[13]H. J. Monkhorst and J. D. Pack, Phys. Rev. B **13**, 5188 (1976).
[14]K. Parlinski, Z.-Q. Li, and Y. Kawazoe, Phys. Rev. Lett. **78**, 4063 (1997).
[15]N. Chetty and M. Weinert, Phys. Rev. B **56**, 10844 (1997).
[16]P. Karen, A. Kjekshus, Q. Huang, and V. L. Karen, J. Alloys Compd. **282**, 72 (1999).
[17]X. Wu, R. Wang, and S. Wang, Appl. Surf. Sci. **256**, 3409 (2009).
[18]Z. P. Luo and S. Q. Zhang, J. Mater. Sci. Lett. **19**, 813 (2000).
[19]A. Datta, U. Ramamurty, S. Ranganathan, and U. V. Waghmare, Comput. Mater. Sci. **37**, 69 (2006).
[20]J. A. Moriarty and A. K. McMahan, Phys. Rev. Lett. **48**, 809 (1982).
[21]J. Xie, S. de Gironcoli, S. Baroni, and M. Scheffler, Phys. Rev. B **59**, 965 (1999).
[22]A. A. Quong and A. Y. Liu, Phys. Rev. B **56**, 7767 (1997).
[23]A. Seko, F. Oba, A. Kuwabara, and I. Tanaka, Phys. Rev. B **72**, 024107 (2005).
[24]S. Minamoto, M. Kato, K. Konashi, and Y. Kawazoe, J. Nucl. Mater. **385**, 18 (2009).
[25]T. Tohei, A. Kuwabara, F. Oba, and I. Tanaka, Phys. Rev. B **73**, 064304 (2006).
[26]G. Kresse, J. Furthmuller, and J. Hafner, Europhys. Lett. **32**, 729 (1995).
[27]J. P. Poirier, *Introduction to the Physics of the Earth's Interior*, 2nd ed. (Cambridge University Press, New York, 2000).
[28]H. J. Gotsis, D. A. Papaconstantopoulos, and M. J. Mehl, Phys. Rev. B **65**, 134101 (2002).
[29]A. Datta, U. V. Waghmare, and U. Ramamurty, Acta Mater. **56**, 2531 (2008).